IEEE Access
Multidisciplinary ⋮ Rapid Review ⋮ Open Access Journal

Received April 14, 2022, accepted May 6, 2022, date of publication May 13, 2022, date of current version May 31, 2022.

Digital Object Identifier 10.1109/ACCESS.2022.3175009

A Cross-Polarisation Discrimination Analysis of Off-Body Channels in Passenger Ferryboat Environments

SŁAWOMIR J. AMBROZIAK[1], (Senior Member, IEEE), KRZYSZTOF K. CWALINA[1], (Member, IEEE), PIOTR RAJCHOWSKI[1], (Member, IEEE), FILIPE D. CARDOSO[2], (Member, IEEE), MANUEL M. FERREIRA[2], (Member, IEEE), AND LUIS M. CORREIA[3], (Senior Member, IEEE)

[1]Faculty of Electronics, Telecommunications and Informatics, Gdańsk University of Technology, 80-233 Gdansk, Poland
[2]ESTSetúbal, Polytechnic Institute of Setúbal and INESC-ID, 2914-508 Setúbal, Portugal
[3]IST/INESC-ID, University of Lisbon, 1000-029 Lisbon, Portugal

Corresponding author: Sławomir J. Ambroziak (slawomir.ambroziak@pg.edu.pl)

This work was performed within the scope of COST Action CA20120, "Intelligence-Enabling Radio Communications for Seamless Inclusive Interactions" (INTERACT).

ABSTRACT There is a need for investigating radio channels for Body Area Networks considering the depolarisation phenomenon and new types of environments, since these aspects are becoming very important for systems design and deployment. This paper presents an analysis of cross-polarisation discrimination for off-body channels based on a measurement campaign performed in a passenger ferryboat, i.e., where all walls, floors and ceilings are made of metal. Firstly, the measurement campaign, including test-bench and scenarios, as well as the analysis approach, including classification of mutual antennas' orientation and definition of parameters are described. The analysis of results includes distance, on-body antennas location and several scenarios, addressing statistical parameters. Mean values for the cross-polarisation discrimination are in the range of [3.7, 6.8] dB while the standard deviation is around 10.0 dB. There is no dependence of the cross-polarisation discrimination on distance, within the measured range (up to 16 m). It is found that there is no correlation between radio signals received by vertically and horizontally polarised receiving antennas, hence, enabling the application of polarisation diversity in Body Area Networks. The Normal Distribution is the best fit for describing cross-polarisation discrimination, as shown by the analysis of goodness of fit parameters, since it passes many of the tests.

INDEX TERMS Body area networks, off-body channels, cross-polarisation discrimination, passenger Ferryboat environments.

I. INTRODUCTION

Body Area Networks (BANs) are small-scaled networks that may operate inside, on, or in the peripheral proximity of a body [1], nowadays being a very promising technology with many possible applications, not only in entertainment and user identification but also in healthcare and medical applications [2]. The design of a BAN (as any other wireless system) should be preceded by a deep analysis of radio channel properties in the target frequency band, environment and scenario, given that power constraints, antennas visibility and mobility, among others, can impose stringent requirements. For this reason, there is an unceasing need for investigating radio channels for new types of systems working in new frequency bands and/or in new types of environments, such as the interior of a passenger ferryboat, where all walls, floors and ceilings are made of metal.

A very important phenomenon in the wireless channel is the depolarisation effect, which yields mismatched polarisations between the receiver (Rx) antenna and the incident electric field coming from the transmitter (Tx) one after being reflected and diffracted on the environment. In general, the

The associate editor coordinating the review of this manuscript and approving it for publication was Gokhan Apaydin.

channel's depolarisation characteristics depend on the environment (i.e., its geometry and electromagnetic properties), radiation/polarisation patterns of antennas and propagation conditions, as well as user's dynamics [3].

This paper refers to the very untypical environment of a passenger ferryboat's interior, with different shapes of scenarios, e.g., rectangular or circular, for which some work can be found in the literature. In [4], system loss measurements in a cabin for static lying users are described and analysed, where the presence of metal surroundings is noticeable. In [5], [6], narrowband (NB) and ultra-wideband (UWB) channel models have been presented. This environment has been also addressed in [7], where the fast fading behaviour of signals for BANs in a circular room has been characterised; a wideband (WB) channel model for the same scenario has been proposed in [8], where the dependence between mean delay and average delay spread on circle radius, frequency and distance between Tx and Rx has been analysed. Still, these works do not account for the depolarisation effect.

In the literature, one can find many works on the depolarisation of signals, but only a minority are related to BANs. For example, in [9] the static NB on-body channel polarisation distribution at 2.4 GHz has been analysed, based on both measurements and simulations; it is shown that a strong depolarisation of on-body channels is more easily caused in a sitting posture, due to the scattering effects from legs.

In [10], a simulation study on the influence of the user's body motion on the polarisation mismatch between the external antenna and different types of wearable ones is presented; it is shown that the performance of NB off-body radio channels at 2.4 GHz depends on both body motion and type of on-body antenna. The influence of human walk on the cross-polarisation ratio is also discussed in [11], [12]; the study is based on simulations performed for on-body channels at 2 GHz, being shown that changes of the cross-polarisation ratio coincide with body motion. An extensive channel model for off-body channels that takes the depolarisation effect and its dependence on users' dynamics into account is proposed in [13]; the analysis shows that, by comparing simulation results between polarised and non-polarised channels in a free space propagation scenario, the difference between the two may be up to 53 dB, which demonstrates how important it is to consider this phenomenon in channel modelling. It should also be noted that the depolarisation effect in the radio channel caused by user motion, e.g., arm-swing, and its influence on channel characteristics may be effectively minimised by the use of a polarisation-controlled active antenna, as shown in [14].

In [15], an experimental investigation of a UWB on-body radio channel with multiple-input–multiple-output (MIMO) antennas for BANs in indoor environments is presented; one of the aspects is the influence of mutual antennas' polarisation on the received power, being shown that the cross-polarised channel may become significant in Non-Line-of-Sight (NLoS) conditions, due to the similar order of magnitude of multi-path components. In [16], [17], a complex geometrical model for polarised WB on-body channels at 13 GHz is proposed; the model is used to prove that channel depolarisation due to ground scattering wave components can be significant and that ground scattering propagation dominates the overall BAN channel behaviour in the investigated conditions. In [3], the depolarisation effect in off-body channels is also studied, based on measurements performed at 2.45 GHz in an indoor environment, and a model for a dynamic off-body channel is proposed, for both co- (CP) and cross-polarised (XP) channels.

So far, to the authors' knowledge, there is no comprehensive research on radio channel modelling addressing polarisation aspects for BANs operating in a harsh reverberating environment as the one of a passenger ferryboat, which constitutes the main difference between already existing work in the literature and the research presented herein. A first approach has been presented in [18], where a preliminary analysis of cross-polarisation discrimination for BANs in a cylindrical room has been performed, presenting an initial analysis for this single scenario and one room type only. The goal of the current paper is to analyse in a deeper perspective the depolarisation effect (based on the cross-polarisation discrimination ratio) in dynamic NB off-body channels operating at 2.45 GHz in several scenarios of a passenger ferryboat, which constitutes novel work, as shown by the review of the state of the art.

The main contributions of this paper are the analysis of general statistics for the cross-polarisation discrimination ratio in the investigated environment, followed by the selection of best fitted probability distributions with the corresponding ranges of parameters. Based on this approach, the rationale for the usage of polarisation diversity in BANs is presented, enabling the use of parameters for system design.

The rest of the paper is structured as follows. Section II describes the measurement campaign, including test-bench and scenarios. The analysis approach, including measurement scenarios, classification of mutual antennas' orientation and definition of parameters, is presented in Section III, and in Section IV the analysis of the cross-polarisation discrimination ratio is performed, including general statistics and dependence on distance. A statistical model is proposed in Section V. The paper is concluded in Section VI.

II. MEASUREMENT CAMPAIGN

This section presents a brief description of the equipment used in the measurements and of the environments where measurements were performed.

A. TEST-BENCH

The measurement campaign has been performed during a cruise of the passenger ferryboat MF-WAWEL on the Baltic Sea, between Gdańsk (Poland) and Nynäshamn (Sweden). The measurements were done with the use of the test-bench presented in [18] and the equipment described in [19], in the configuration suitable to obtain system loss for BANs with a polarisation discrimination scheme.

The measurement stand was divided into three sections: control, executive and antennas. The control section consisted of a portable computer with dedicated software, responsible for controlling the whole test-bench, via the local area network and switch, and for data registration and storage. The executive section consisted of the vector signal generator, R&S SMU200A [20], acting as the Tx, and two digital wideband Rxs, R&S EM550 [21], working synchronously, capturing the power of the signal with a variable period between measurements, with an average of 3.9 ms and a standard deviation of 3.2 ms. The antennas section had an on-body rectangular patch Tx antenna (with a 3 dBi gain, linear vertical polarisation and half-power beamwidths of 140° and 115° in the E- and H-planes, respectively) and a dual-polarised Rx one, LB-OSJ-0760 [22] (with a 10 dBi gain and half-power beamwidths, of 58° and 46° in the E- and H-planes, respectively). The height of the Rx antenna centre was 1.3 m regardless of the scenario, while the Tx one was mounted on three locations of the user's body, Figure 1:

- right side of the head-HE_R (at the height of 1.6 m);
- front side of the torso-TO_F (at the height of 1.3 m);
- bottom part of the left arm-AB_L (at the height of 0.9 m).

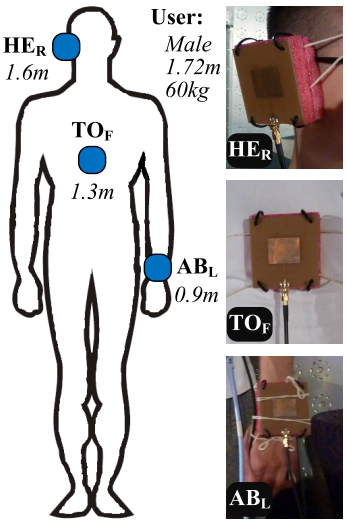

FIGURE 1. Tx on-body antenna placements and heights.

All RF connections were made with Sucoflex 126E cables [23], each with a length of 10 m and total attenuation of 4 dB (taken under consideration during the calibration process).

One should note that the on-body Tx antenna has a hemispherical radiation pattern with a gain in the body direction about −30 dBi, hence, given that the power at the input of the Tx antenna was 0 dBm, the power radiated into the body was about −30 dBm, which presents no risk.

B. ENVIRONMENT

Measurements have been performed on decks 7 (71.26 m long × 22.24 m wide) and 8 (63.64 m long × 22.24 m wide), in rooms with different shapes and dimensions, i.e., a corridor corner (CoCo), a straight corridor (StCo) and a disco (Disc), Figures 2 and 3. It should be stressed that the majority of the construction elements in this environment (e.g., walls, floor, ceiling and doors) are made of steel with different thicknesses. In some places there are also additional elements and objects, such as floor covering, fire extinguishers or fire bells, but, in general, all rooms may be considered as reverberating environments with different dimensions.

The CoCo scenario consisted of two perpendicular subsections of straight corridors (around 10 m long) with a height of 2 m and a width of 1 m and 1.8 m, respectively; there is a kind of cavity in the wider corridor, which may be seen at the top right part of Figure 3, its dimensions being around 1.9 × 2.0 × 2.0 m^3. On the other hand, StCo is a selected section (20 m long) of the longer corridor with a width of 1 m and a height of 2 m. The most untypical room is Disc, which is an indoor environment with a cylindrical shape (16 m diameter) and hemispherical ceiling (7.3 m high at the middle).

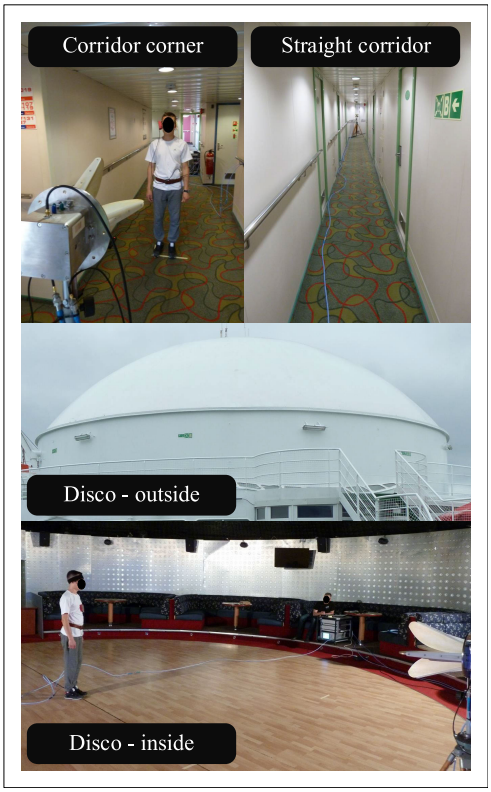

FIGURE 2. View of the measured environments.

III. ANALYSIS APPROACH

In this section, one presents the approach taken for the analysis, including measured scenarios, classification of mutual antennas' orientation and definition of parameters.

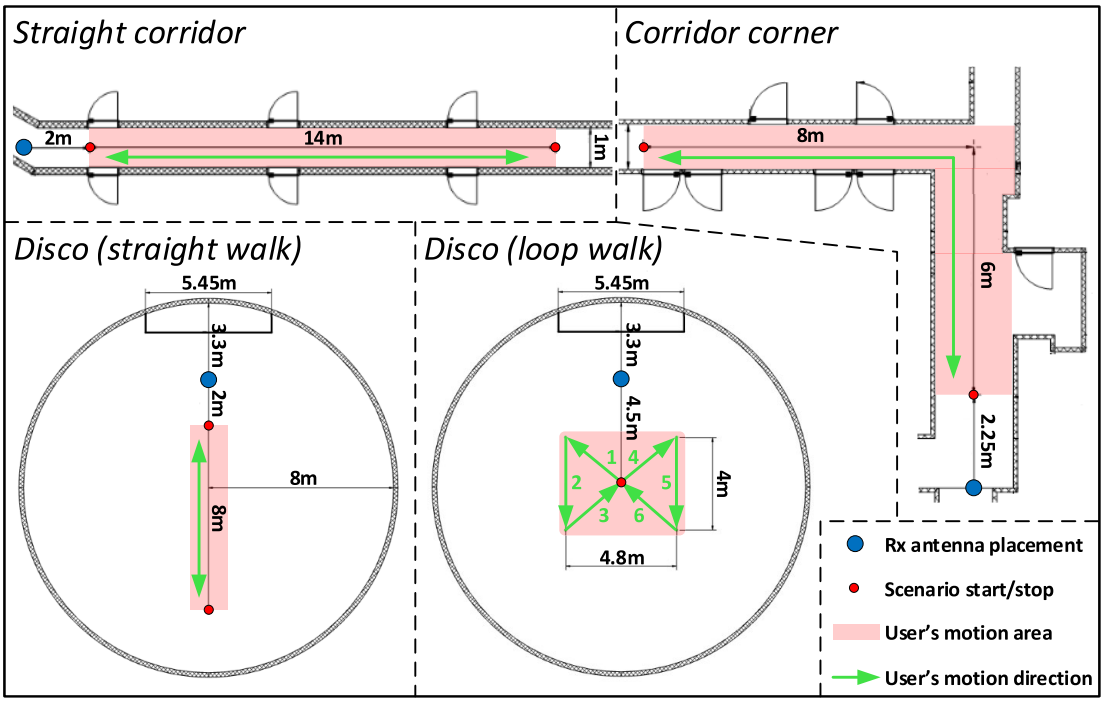

FIGURE 3. Geometry of the measured environments.

A. SCENARIOS

The measured environments are sketched in Figure 3, where the Rx off-body antenna placement is marked with a blue dot, path starting and ending points are marked with red dots, user motion's area is indicated by a light red polygon, and user motion's direction is indicated by light green arrows.

In each environment, measurements were carried out for two dynamic scenarios regarding user motion relative to the Rx antenna, approaching (A) and departing (D), with an approximate constant speed. These two scenarios are widely considered in BANs research. as they allow for the analysis of the measurement data independently of the side of the body on which the node is located, e.g., regardless of the antenna's placement on the left or right wrists. For Scenario D, the user started his walk at 2 m from the Rx antenna (to ensure that the user was in its far field, which is around 1.6 m) and walked towards the end point. Scenario A is reversed with respect to the previous one, i.e., walking the same path in the opposite way. The walking distance was 14 m for StCo and CoCo, and 8 m for the straight walk in Disc. Additionally, a loop walk scenario (L) was performed in Disc, with the user walking with an approximate constant speed along an hourglass-shaped route having the starting point at 4.5 m from the Rx antenna, Figure 3, the dimensions of the walking area being 4.0×4.8 m^2.

In order to obtain a large enough set of data, containing information about the time variant characteristics of the propagation channel, measurements were repeated 10 times for each scenario and on-body antenna placement, allowing to obtain a total of 74 648 samples. The number of measurements for each particular environment and scenario is summarised in Table 1.

TABLE 1. No. of measurements for particular environments and scenarios.

Environment	Scenario	No. of meas.
Straight corridor - StCo	A	10 689
	D	10 989
Corridor corner - CoCo	A	11 615
	D	11 949
Discotheque - Disc	A	5 853
	D	6 499
	L	17 054
	Total	74 648

It should be also mentioned that during measurements there were no other people inside the corridors or the disco room, besides the user and the test-bench operator.

B. MUTUAL ANTENNAS' ORIENTATION

In the majority of the investigated cases, the direct line between user and Rx antenna was not obstructed, being considered as a Line-of Sight (LoS) situation. In the case of CoCo, this line is obstructed by the metallic walls when the user is behind the corner, so one can consider this case as a NLoS. On the other hand, as system loss strongly depends on the mutual orientation of both antennas in the radio link, which has been proved in [24], [25], three cases can be considered for the on-body antenna orientation [19], [25]:

- Co-Directed (CD)—when the maximum gain of one antenna is directed towards the other one (only Scenario A TO_F);

- Opposite-Directed (OD)—when the maximum gain of one antenna is directed in the opposite direction to the other one (only Scenario D TO_F);
- Cross-Directed (XD)—when the maximum gain of one antenna is directed in an orthogonal direction to the other one (both Scenarios A and D with HE_R and AB_L).

In the case of the loop walk in the disco room, Scenario L, it is difficult to determine the mutual orientation of both antennas, so one may assume it is random, i.e., case R.

Regarding the direct visibility between the user and the Rx antenna, by considering the mutual orientation of the two antennas, one can distinguish the following cases:

- LoS-Co-Directed (LoS, CD);
- LoS-Opposite-Directed (LoS, OD);
- LoS-Cross-Directed (LoS, XD);
- NLoS-Co-Directed (NLoS, CD);
- NLoS-Opposite-Directed (NLoS, OD);
- NLoS-Cross-Directed (NLoS, XD).

Cases (NLoS, CD) and (NLoS, OD) refer to the on-body antenna being directed towards the corner and in the opposite way, respectively.

C. PARAMETERS USED IN THE ANALYSIS

There is a vast number of parameters that can be used to assess the fitting of a statistical distribution to a set of observed data, which usually may indicate different aspects of the data, of the distribution or both. The selection of parameters has been done according to the use of the statistical tools that have taken in the paper, being the χ^2 test, the coefficient of determination R^2 and the correlation coefficient r_{VH}.

The cross-polarisation discrimination ratio (X_{PD}) is considered for the depolarisation effect analysis, being defined as the ratio between the Rx powers received in the CP and XP channels, respectively [3], [26]. For a given linear vertical polarisation of the Tx antenna, X_{PD} is calculated by:

$$X_{PD[\mathrm{dB}]} = P^{V}_{r[\mathrm{dBm}]} - P^{H}_{r[\mathrm{dBm}]}, \tag{1}$$

where P^V_r and P^H_r are the powers received by the vertical and horizontal polarised Rx antennas, respectively, i.e., the CP and XP channels.

For the evaluation of the average behaviour of X_{PD} in different scenarios, the mean (μ_X) and median (m_X) values have been analysed, while its dispersion has been analysed via the standard deviation (σ_X), which are well-known parameters [27], [28]. Additionally, the minimum ($X_{PD,min}$) and maximum ($X_{PD,max}$) values have been analysed, in order to have an estimation of the range of variation. The calculation of all these parameters has been based on measurement data obtained for 10 runs for each scenario.

Both linear and log X_{PD} model parameters for the single run of each scenario have been obtained with the use of a linear regression with the least-squares method, after which the average of each parameter over 10 runs has been calculated. The evaluation of the coefficient of determination (R^2) has been used, where $R^2 \in [0, 1]$, [29]: when $R^2 = 1$, the model perfectly fits measurement data, whereas when $R^2 = 0$ there is no relationship between the dependent variable (response of the model) and independent variables (predictors); in general, R^2 gives the percentage of variance in the dependent variable that can be explained by the independent variables used in the model [6].

The distance between two successive measurement samples was calculated according to the average speed of the user for each of the scenario runs, varying between 0.9 m/s and 1.2 m/s, with an overall average of 1 m/s.

The establishment of a statistical model for X_{PD} consisted of fitting the Probability Distribution Function (PDF) to empirical data and of estimating the corresponding parameters. MATLAB's *fitdist* built-in function [30] has been used, based on the maximum-likelihood parameter estimation. In addition, the χ^2 test (with a significance level of 1%) and correlation coefficient, r, [28], [31] were used as a goodness of fit (GoF) metrics. The χ^2 test gives an absolute measure that indicates if the evidence that samples follow a particular distribution is significant enough. Similarly as for general statistical parameters, samples for all 10 runs of each scenario have been put together for distribution fitting.

The correlation coefficient between powers received at vertical and horizontal polarisations, r_{VH}, has also been used to verify if polarisation diversity may be used in off-body communications. It has been calculated for all 10 runs of each scenario, combined one after another.

IV. ANALYSIS OF THE RESULTS

This section consists of the full analysis of the measurements results, including the general statistical analysis of X_{PD} and its dependence on the distance, d, between user and off-body antennas, and its statistical model.

A. GENERAL STATISTICAL ANALYSIS OF X_{PD}

The general statistics for the LoS case in three different environments, and for the different mutual antennas' orientations, are presented in Tables 2-4.

TABLE 2. General statistics for (StCo, LoS).

Ant. orientation	CD	OD	XD			
Ant. placement	TO_F		HE_R		AB_L	
Scenario	A	D	A	D	A	D
μ_X [dB]	8.7	7.2	2.8	3.0	5.5	2.7
m_X [dB]	8.6	7.1	2.6	3.0	5.3	2.7
σ_X [dB]	10.4	9.6	9.8	10.2	9.9	10.5
$X_{PD,min}$ [dB]	-44.6	-47.1	-43.1	-51.1	-56.4	-65.9
$X_{PD,max}$ [dB]	76.8	58.2	58.6	67.8	69.2	61.1
r_{VH}	-0.04	-0.03	0.02	-0.01	0.01	-0.01

The highest mean values of X_{PD} were obtained for the CD case, being 8.7 dB for StCo (1 m width), 11.2 dB for CoCo (1.8 m width) and 14.3 dB for Disc (8 m radius); these values somehow increase with the dimensions of the room. For the OD case the behaviour is different and the values are quite similar, i.e., 7.2 dB, 7.4 dB and 7.4 dB, respectively for StCo, CoCo and Disc. The lowest values were obtained for the XD

TABLE 3. General statistics for the (CoCo, LoS).

Ant. orientation	CD	OD	XD			
Ant. placement	TO_F		HE_R		AB_L	
Scenario	A	D	A	D	A	D
μ_X [dB]	11.2	7.4	2.9	3.6	6.0	4.8
m_X [dB]	11.3	7.1	2.7	3.5	6.0	5.1
σ_X [dB]	10.2	9.7	10.4	9.8	10.4	10.0
$X_{PD,min}$ [dB]	-38.9	-49.5	-55.8	-53.8	-56.8	-58.6
$X_{PD,max}$ [dB]	64.8	58.8	59.6	52.7	58.5	53.8
r_{VH}	-0.07	0.01	0.00	-0.01	-0.02	0.00

TABLE 4. General statistics for (Disc, LoS).

Ant. orientation	CD	OD	XD			
Ant. placement	TO_F		HE_R		AB_L	
Scenario	A	D	A	D	A	D
μ_X [dB]	14.3	7.4	0.2	1.4	3.5	3.5
m_X [dB]	14.6	7.1	-0.1	1.6	3.5	3.7
σ_X [dB]	9.8	9.4	10.2	9.9	10.2	9.9
$X_{PD,min}$ [dB]	-36.1	-43.1	-50.2	-47.1	-55.1	-50.0
$X_{PD,max}$ [dB]	63.9	57.2	56.7	56.7	58.5	61.5
r_{VH}	0.09	0.06	-0.01	0.01	0.04	0.04

case, ranging in [2.7,5.5] dB for StCo, [2.9,6.0] dB for CoCo and [0.2,3.5] dB for Disc. From these values, one confirms that the presence of a strong direct component (LoS, CD) leads to a strong component at the Rx of the CP signal and a low one for XP; the XP component originates most probably from multiple reflections and diffractions on surrounding metallic surfaces, which create a kind of waveguide (for StCo and CoCo) or reverberation (for Disc) effects. In the OD case, there is also a quite strong CP component, which comes from reflections on the opposite wall, being shadowed only by the user's body. One can also notice that median values are very close to mean ones, the difference not exceeding 0.3 dB, which may indicate that X_{PD} follows a Normal Distribution. Also, the mean value is always positive, which means that, on average, the power of the CP component of the received signal is higher than the XP one, as expected.

When one considers the standard deviation, there is no real difference among the three cases for antennas visibility, all ranging in [9.4,10.5] dB. Also, X_{PD} minimum and maximum values do not show a strong trend with antennas visibility, although maximum $X_{PD,min}$ values tend to occur for TO_F (regardless of CD or OD) and minimum ones for AB_L, and maximum $X_{PD,max}$ values occur for (CD, TO_F). Being clear that these maximum and minimum values are not significant from the statistical viewpoint, they confirm the importance of a strong direct component to obtain a signal with high CP and low XP components. On the other hand, this range of values for X_{PD} hints that polarisation diversity may be successfully used in this type of channels.

The correlation r_{VH} observed in all cases presents quite low values, absolute maxima being obtained for (CD, TO_F), and the largest of all being 0.09; on the other hand, absolute minima are close to 0 (even 0.00). It is usually assumed that an absolute correlation lower than 0.5 enables a proper diversity scheme, [32], hence, one can conclude that polarisation diversity can be used in this type of environments, with very high gains. An example of the received signals on

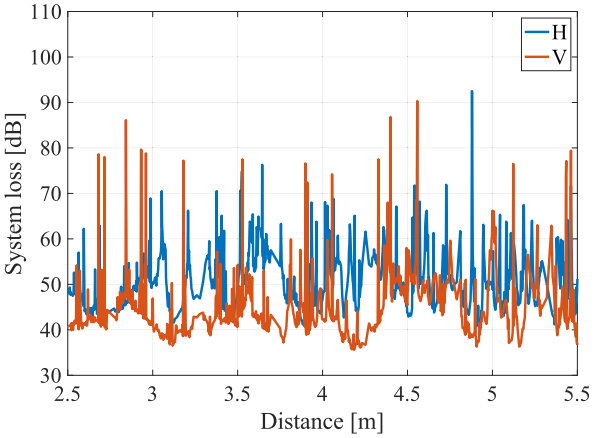

FIGURE 4. System loss vs. distance for (CoCo, LoS, XD, AB_L, D).

TABLE 5. General statistics for (CoCo, NLoS).

Ant. orientation	CD	OD	XD			
Ant. placement	TO_F		HE_R		AB_L	
Scenario	A	D	A	D	A	D
μ_X [dB]	2.1	0.9	2.3	3.4	2.3	1.6
m_X [dB]	1.9	1.0	2.4	3.4	2.3	1.8
σ_X [dB]	10.0	10.3	10.6	9.8	10.6	10.3
$X_{PD,min}$ [dB]	-63.8	-57.3	-58.7	-59.2	-60.3	-62.5
$X_{PD,max}$ [dB]	65.8	54.1	64.6	59.7	56.9	63.3
r_{VH}	0.07	-0.02	0.31	0.19	0.01	0.06

both polarisations is presented in Figure 4 for (CoCo, LoS, XD, AB_L, D) in a single measurement run, where indeed the V- and H-polarised signals show a strong uncorrelation, deep fades occurring at different distances/times.

When one considers the situations in which only NLoS occurs, Table 5, the mean values of X_{PD} (also being close to medians) are significantly lower for CD (by 9.1 dB) and OD (by 6.5 dB), due to the lack of a strong component, while no major difference exists for XD, which is also due to the additional depolarisation of the signal that propagates behind the corner. On the other hand σ_X values are very similar to the ones measured in LoS. Minimum and maximum values of X_{PD} are also comparable to LoS ones.

The maximum of r_{VH}, 0.31, was obtained for (CoCo, NLoS, XD, HE_R, A), but it is still low enough so that signals can be considered uncorrelated, hence, even in this case, one can aim at using polarisation diversity. Figure 5 shows one of the runs for this worst case, where it is visible that the occurrence of deep fades does not happen at the same time.

B. X_{PD} DEPENDENCE ON DISTANCE

In order to examine the dependence of X_{PD} on distance, d, both linear and log models have been investigated, i.e.,

$$X_{PD[\mathrm{dB}]} = A_{lin[\mathrm{dB/m}]} \cdot d_{[\mathrm{m}]} + B_{lin[\mathrm{dB}]}, \quad (2)$$

$$X_{PD[\mathrm{dB}]} = 10A_{log} \cdot \log\left(d_{[\mathrm{m}]}/d_{0[\mathrm{m}]}\right) + B_{log[\mathrm{dB}]}, \quad (3)$$

where parameters A_{lin} and B_{lin} refer to the linear model and A_{log} and B_{log} to the log one ($d_0 = 1$ m). The coefficient of determination, R^2, takes very low values in both approaches, being in the range of [0.00, 0.14] and of [0.00, 0.13] for

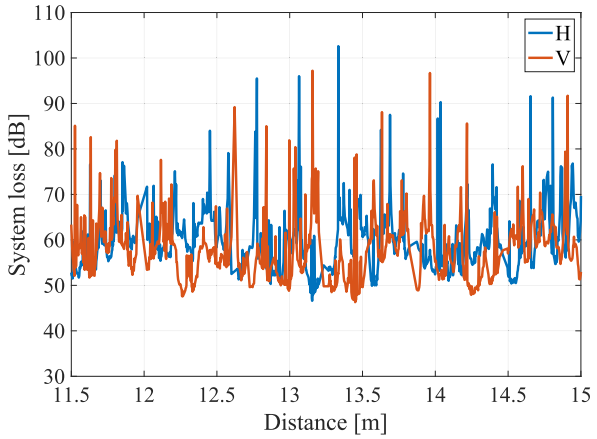

FIGURE 5. System loss vs. distance for (CoCo, NLoS, XD, HE_R, A).

the linear and log models, respectively. These very similar results show that there is no real relationship between cross-polarisation discrimination and distance, for the measured environments and scenarios.

C. X_{PD} ANALYSIS FOR THE LOOP SCENARIO

Since in Scenario L the user did not perform a straight walk, for which the mutual orientation of both antennas can be considered random, this case is analysed separately. This scenario seems to be somehow the most natural situation, when the position of the user in the environment does not follow a straight line and mutual antennas' orientations are a mixture of different possibilities.

The general statistics are presented in Table 6. For the Tx antenna placed on TO_F and HE_R, mean and median values are similar, between 6.4 dB and 6.8 dB, being quite lower for AB_L (around 3.6 dB). The first two positions are the more stable ones, while the last one is definitely more dynamic, hence, again showing that the location of the antennas on the body and the dynamicity of that location impacts on polarisation discrimination, i.e., regarding the use of polarisation diversity in BANs, some locations on the body tend to yield better results than others.

The standard deviation is comparable with the previous A and D scenarios. A behaviour similar to previous cases is observed for r_{VH}, with a maximum 0.17, hence, making it possible to extend the conclusions of previous scenarios to this one. Concurrently, no dependence on distance is obtained, R^2 not exceeding 0.01.

A plot of X_{PD} for one of the runs with the Tx antenna placed on TO_F is presented in Figure 6. The graph has been divided into six parts, corresponding to the path sections shown in Figure 3. The average clearly changes while the user walks along the loop: in sections 2 and 5 (OD case), a more stable curve seems to be observed, while one can see an increasing trend for sections 3 and 6 (CD case); on the other hand, when the user passes the start/stop point (red dot in Figure 3), i.e., sections 1 and 4, the visibility changes to XD, leading to a decreasing trend.

TABLE 6. General statistics (Disc, LoS, R).

Ant. orientation	R		
Ant. placement	TO_F	HE_R	AB_L
Scenario	Loop walk		
μ_X [dB]	6.5	6.8	3.7
m_X [dB]	6.4	6.7	3.6
σ_X [dB]	10.0	9.6	10.0
$X_{PD,min}$ [dB]	-46.1	-56.0	-53.4
$X_{PD,max}$ [dB]	60.1	61.1	59.3
r_{VH}	0.06	0.05	0.17

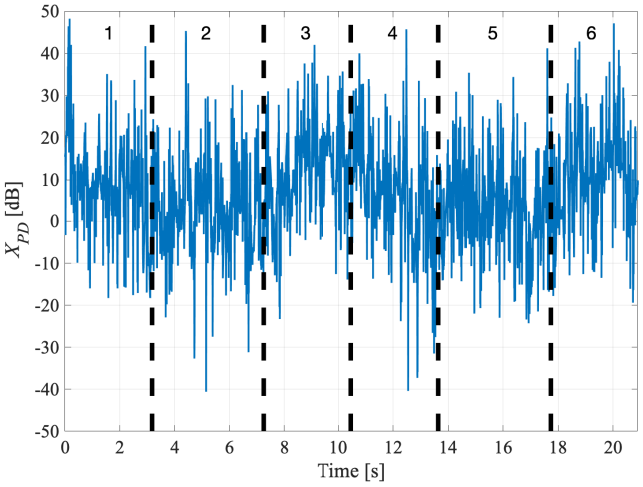

FIGURE 6. X_{PD} vs. time for the loop walk scenario (Disc, L, TO_F).

One should note that this kind of cylindrical environment presents different catacaustic regions, depending on the number of multipath components, [7], which may cause different fading behaviours of the V- and H-polarised signals.

V. STATISTICAL MODELLING

This section addresses the modelling of X_{PD} statistical behaviour, by fitting a distribution to data, which is useful for the choice of the location of wearables on the body and for system design, including the use of polarisation diversity.

The previous analysis of X_{PD} allows one to assume that the Normal Distribution should be used for this purpose, so this distribution was taken for the fitting process, $X_{PD} \sim N(\mu, \sigma)$. Tables 7-11 show the distribution parameters for all cases, as well as the metrics taken for fitting assessment; one has $\chi^2_{crit} = 72.4$, for a 1% significance level. The Normal Distribution seems to be indeed a good one to be taken to describe the behaviour of X_{PD} with an acceptable accuracy in a good number of cases: the correlation coefficient is always very close to 1, i.e., $r \in [0.97, 0.99]$, but χ^2 is higher than χ^2_{crit} in many cases. There is a situation where the χ^2 test fails in all cases, (CoCo, LoS), for which results are presented in Figure 7, where one can see that the behaviour is still similar to a Normal Distribution, although not being a good fit (the other non-fitting cases present similar curves). The worst fits tend to be the (LoS, TO_F) cases, namely Scenario A, while (LoS, HE_R) can be considered reasonable fitted, and NLoS provides a good fit in all cases. In fact, the existence of LoS

TABLE 7. Distribution parameters for (StCo, LoS).

Ant. orientation	CD	OD	XD			
Ant. placement	TO_F		HE_R		AB_L	
Scenario	A	D	A	D	A	D
μ [dB]	8.7	7.2	2.8	3.0	5.5	2.7
σ [dB]	10.4	9.6	9.8	10.2	9.9	10.5
r	0.98	0.99	0.98	0.98	0.98	0.97
χ^2	188.5	159.1	73.2	74.3	108.7	65.0

TABLE 8. Distribution parameters for (CoCo, LoS).

Ant. orientation	CD	OD	XD			
Ant. placement	TO_F		HE_R		AB_L	
Scenario	A	D	A	D	A	D
μ [dB]	11.2	7.4	2.9	3.6	6.0	4.8
σ [dB]	10.2	9.7	10.4	9.8	10.4	10.0
r	0.98	0.97	0.97	0.98	0.97	0.97
χ^2	298.4	164.3	72.7	79.0	112.6	89.5

TABLE 9. Distribution parameters for (Disc, LoS).

Ant. orientation	CD	OD	XD			
Ant. placement	TO_F		HE_R		AB_L	
Scenario	A	D	A	D	A	D
μ [dB]	14.3	7.4	0.2	1.4	3.5	3.5
σ [dB]	9.8	9.4	10.2	9.9	10.2	9.9
r	0.97	0.97	0.97	0.98	0.98	0.98
χ^2	620.3	169.2	47.4	57.7	81.3	76.1

TABLE 10. Distribution parameters for (CoCo, NLoS).

Ant. orientation	CD	OD	XD			
Ant. placement	TO_F		HE_R		AB_L	
Scenario	A	D	A	D	A	D
μ [dB]	2.1	0.9	2.3	3.4	2.3	1.6
σ [dB]	10.0	10.3	10.6	9.8	10.6	10.3
r	0.98	0.98	0.97	0.98	0.97	0.98
χ^2	60.4	52.9	65.2	75.8	61.5	59.3

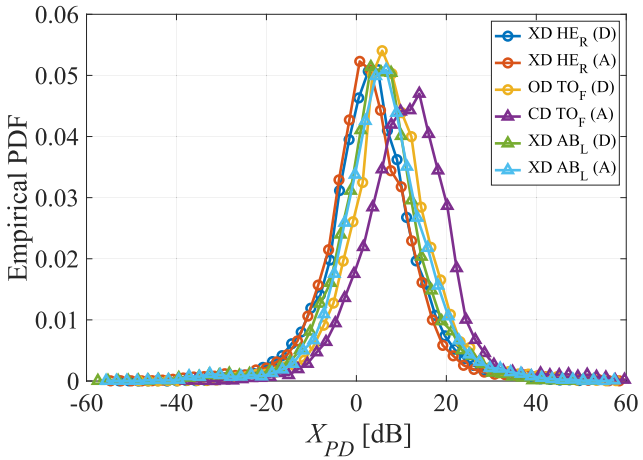

FIGURE 7. Empirical distribution of X_{PD} for (CoCo, LoS).

leads to a strong CP component, which may "disturb" the approximation by the Normal Distribution, while NLoS tends to be closer to the more random situation.

TABLE 11. Distribution parameters for (Disc, LoS, L).

Ant. orientation	R		
Ant. placement	TO_F	HE_R	AB_L
Scenario	L		
μ [dB]	6.5	6.8	3.7
σ [dB]	10.0	9.6	10.0
r	0.99	0.98	0.99
χ^2	136.5	148.0	79.3

In conclusion, one can state that X_{PD} can be described by a Normal Distribution for the several environments that one can find in a passenger ferryboat, being a better fit for NLoS situations and for lower mobility, for which $\mu \in [2.8, 14.3]$ dB and $\sigma \in [9.4, 10.6]$ dB regardless of the particular scenario; μ tends to take higher values for antennas in lower mobility locations and LoS (i.e., TO_F in CD), lower ones occurring for NLoS where mobility does not have such strong impact.

VI. CONCLUSION

This paper presents an analysis of cross-polarisation discrimination, X_{PD}, in off-body channels based on measurements performed in passenger ferryboat environments, i.e., where all walls, floors and ceilings are made of metal. One starts by giving the framework within which the work has been performed, followed by a review of the state of the art. Then, the measurement campaign is described, including the measurement stand and investigated environments. The approach to the analysis is provided, including measurement scenarios, classification of mutual antennas' orientation and definition of parameters used in the analysis.

Measurements have been performed in rooms with different shapes and dimensions, i.e., the corner of a corridor, a straight corridor and a disco. In each environment, measurements were carried out for two dynamic scenarios regarding user motion, i.e., approaching and departing, with an approximate constant speed, and in addition, in the disco one, a loop walk was performed. The Rx antenna was a dual-polarised fixed one, while the Tx one was mounted on three locations of the user's body: right side of the head, front side of the torso and bottom part of the left arm. Three cases were considered for the on-body antenna orientation: Co-Directed, when the maximum gain of one antenna is directed towards the other one; Opposite-Directed, when the maximum gain of one antenna is directed in the opposite direction to the other one; and Cross-Directed, when the maximum gain of one antenna is directed in an orthogonal direction to the other one. In addition Line-of-Sight and Non-Line-of-Sight are considered. Measurements were repeated 10 times for each scenario and on-body antenna placement, allowing to obtain a total of 74 648 samples for the cross-polarisation discrimination ratio.

The analysis of results for X_{PD} includes the general statistics and the dependence on the distance. Mean values for X_{PD} are in the range of [3.7, 6.8] dB while the standard deviation is around 10.0 dB. The maximum correlation between vertical and horizontal components is 0.31, which is low enough so that signals can be considered uncorrelated, hence, one can

aim at using polarisation diversity in Body Area Networks. There is no dependency of X_{PD} on distance, within the measured range (up to 16 m). The Normal Distribution is found to be an acceptable fit to describe X_{PD}, since the metrics taken for the goodness of fit pass the test in many cases. The average ranges in [2.8, 14.3] dB and the standard deviation in [9.4, 10.6] dB regardless of the particular scenario, but the former tends to take higher values for antennas in lower mobility locations and LoS, lower ones occurring for NLoS where mobility does not have such strong impact.

It should be noted that, since there are no other comprehensive analyses for BANs operating in a ferryboat environment and taking the depolarisation phenomenon into account, one can expect that the proposed statistical models are more effective for this environment than others that have been developed for other conditions.

This paper deals with the analysis of data originated from measurements and the establishment of fitting statistical distributions to these data. Hence, the obtained results are associated with the environment that has been measured and the antennas that have been used in the measurements, and extrapolation has to be done with care. Regarding the former, indeed, other types of environments, namely those that are not almost entirely covered with metallic surfaces, may lead to quite different results, but this difference is expected to be more in the range of values for the parameters rather than in the statistical distributions, which are well known good fitting ones for this purpose; as far as the latter are concerned, given that the targeted applications are those in BANs, where antennas located on the body usually have a radiation pattern of the hemispheric type, as the ones used in the measurements, one should not expect that large differences will occur for other cases. In any case, the research plan of the authors includes the use of other types of antennas, so that this kind of dependence can be better understood.

REFERENCES

[1] H.-B. Li, K. Yazdandoost, and B. Zhen, *Wireless Body Area Network*. Aalborg, Denmark: River Publishers, 2010.

[2] J. Wang and Q. Wang, *Body Area Communications—Channel Modeling, Communication Systems, and EMC*. Singapore: Wiley, 2013.

[3] K. Turbic, S. J. Ambroziak, and L. M. Correia, "Characteristics of the polarised off-body channel in indoor environments," *EURASIP J. Wireless Commun. Netw.*, vol. 2017, no. 1, pp. 1–15, Oct. 2017.

[4] P. T. Kosz, S. J. Ambroziak, and L. M. Correia, "Radio channel measurements in off-body communications in a ferry passenger cabin," in *Proc. 32nd Gen. Assem. Sci. Symp. Int. Union Radio Sci. (URSI GASS)*, Montreal, QC, Canada, Aug. 2017, pp. 1–4.

[5] K. Cwalina, S. Ambroziak, and P. Rajchowski, "An off-body narrowband and ultra-wide band channel model for body area networks in a ferryboat environment," *Appl. Sci.*, vol. 8, no. 6, p. 988, Jun. 2018.

[6] M. Laskowski, S. J. Ambroziak, L. M. Correia, and K. Swider, "On the usefulness of the generalised additive model for mean path loss estimation in body area networks," *IEEE Access*, vol. 8, pp. 176873–176882, 2020.

[7] F. D. Cardoso, P. T. Kosz, M. M. Ferreira, S. J. Ambroziak, and L. M. Correia, "Fast fading characterization for body area networks in circular metallic indoor environments," *IEEE Access*, vol. 8, pp. 43817–43825, 2020.

[8] F. D. Cardoso, M. M. Ferreira, S. J. Ambroziak, and L. M. Correia, "A wideband channel model for body area networks in circular metallic indoor environments," *IEEE Access*, vol. 9, pp. 73791–73798, 2021.

[9] L. Liu, P. Zhang, X. Wang, X. Zhang, and N. Jiang, "Analysis of static narrowband on-body channel polarization distribution at 2.4 GHz," *Int. J. Antennas Propag.*, vol. 2018, pp. 1–10, Oct. 2018.

[10] K. Y. Yazdandoost and R. Miura, "Antenna polarization mismatch in BAN communications," in *Proc. IEEE MTT-S Int. Microw. Workshop Ser. RF Wireless Technol. Biomed. Healthcare Appl. (IMWS-BIO)*, Singapore, Dec. 2013, pp. 1–3.

[11] K. Li, K. Honda, and K. Ogawa, "Analysis of the body proximity cross-polarization power ratio in a human walking motion," in *Proc. Int. Workshop Electromagnetics, Appl. Student Innov. Competition (iWEM)*, Hsinchu, Taiwan, Nov. 2015, pp. 1–2.

[12] K. Li, K. Honda, and K. Ogawa, "Analysis of the body proximity cross-polarization power ratio in a human walking motion," in *Proc. Asia–Pacific Microw. Conf. (APMC)*, Nanjing, China, Dec. 2015, pp. 1–3.

[13] K. Turbic, L. M. Correia, and M. Beko, "A channel model for polarized off-body communications with dynamic users," *IEEE Trans. Antennas Propag.*, vol. 67, no. 11, pp. 7001–7013, Nov. 2019.

[14] K. Li, K. Honda, and K. Ogawa, "Experiments of a polarization-controlled active antenna to enhance BAN on-body link in human dynamic channels," in *Proc. 9th Int. Symp. Med. Inf. Commun. Technol. (ISMICT)*, Kamakura, Japan, Mar. 2015, pp. 117–120.

[15] W.-J. Chang, J.-H. Tarng, and S.-Y. Peng, "Frequency-space-polarization on UWB MIMO performance for body area network applications," *IEEE Antennas Wireless Propag. Lett.*, vol. 7, pp. 577–580, 2008.

[16] S. Kwon, G. L. Stüber, A. V. López, and J. Papapolymerou, "Geometrically based statistical model for polarized body-area-network channels," *IEEE Trans. Veh. Technol.*, vol. 62, no. 8, pp. 3518–3530, May 2013.

[17] S.-C. Kwon, G. Stüber, A. Lopez, and J. Papapolymerou, "Polarized channel model for body area networks using reflection coefficients," *IEEE Trans. Veh. Technol.*, vol. 64, no. 8, pp. 3822–3828, Aug. 2015.

[18] S. J. Ambroziak, K. Cwalina, and P. Rajchowski, "The analysis of cross-polarisation discrimination for body area networks in cylindrical metallic environment," in *Proc. 15th Eur. Conf. Antennas Propag. (EuCAP)*, Dusseldorf, Germany, Mar. 2021, pp. 1–3.

[19] S. J. Ambroziak, "Measurement stand and methodology for research of the off-body and body-to-body radio channels in WBANs with different diversity schemes," *Int. J. Antennas Propag.*, vol. 2019, pp. 1–16, Apr. 2019.

[20] *SMU200A Vector Signal Generator*, Rohde&Schwarz, Munich, Germany, 2021. Accesses: Dec. 31, 2021. [Online]. Available: https://scdn.rohde-schwarz.com/ur/pws/dl_downloads/dl_common_library/dl_brochures_and_datasheets/pdf_1/SMW200A_dat-sw_en_3606-8037-22_v1600.pdf

[21] *VHF/UHF Digital Wideband Receiver R&S EM550*, Rohde&Schwarz, Munich, Germany, 2006. Accesses: Dec. 31, 2021. [Online]. Available: https://pdf.directindustry.com/pdf/rohde-schwarz/r-s-em550-vhf-uhf-digital-wideband-receiver-data-sheet/9019-413475.html

[22] A-Info, Irvine, CA, USA. *LB-OSJ-0760 Dual Polarised Quad-Ridged Horn Antenna*. Accessed: Dec. 31, 2021. [Online]. Available: https://www.ainfoinc.com/antenna-products/horn-antennas/dual-polarization-horn-antennas/open-boundary-quad-ridged-horn-antenna/lb-osj-0760-sf-open-boundary-quad-ridged-dual-polarization-horn-antenna-0-7-6-ghz-11db-gain-sma-female

[23] HUBER+SUHNER. *SUCOFLEX 100: Flexible Microwave Cable*. Accesses: Dec. 31, 2021. https://www.ecatalog.hubersuhner.com/material/85020264.

[24] M. Mackowiak, "Modelling MIMO systems in body area networks in outdoors," Ph.D. dissertation, IST-Univ. Lisbon, Lisbon, Portugal, 2013.

[25] M. Mackowiak and L. M. Correia, "Modelling dynamic body-to-body channels in outdoor environments," in *Proc. 31st URSI General Assembly Sci. Symp. (URSI-GASS)*, Beijing, China, Aug. 2014, pp. 1–2.

[26] *Definitions of Terms Relating to Propagation in Non-Ionized Media, International Telecommunication Union—Radiocommunication Sector*, document ITU-R, P.310-9, Geneva, Switzerland, Aug. 2019. Accesses: Dec. 31, 2021. [Online]. Available: https://www.itu.int/dms_pubrec/itu-r/rec/p/R-REC-P.310-10-201908-I!!PDF-E.pdf

[27] R. M. Gray and L. D. Davisson, *An Introduction to Statistical Signal Processing*. Cambridge, U.K.: Cambridge Univ. Press, 2004.

[28] T. T. Soong, *Fundamentals of Probability and Statistics for Engineers*. West Sussex, U.K.: Wiley, 2004.

[29] R. A. Johnson and D. W. Wichern, *Applied Multivariate Statistical Analysis*. Upper Saddle River, NJ, USA: Prentice-Hall, 1988.

[30] *MATLAB*. Accessed: Oct. 6, 2021. [Online]. Available: http://www.mathworks.com

[31] A. M. Mathai and P. N. Rathie, *Probability and Statistics*. London, U.K.: Palgrave Macmillan, 1977.

[32] Y. Huang and K. Boyle, *Antennas: From Theory to Practice*. Chichester, U.K.: Wiley, 2008.

SŁAWOMIR J. AMBROZIAK (Senior Member, IEEE) was born in Poland, in 1982. He received the M.Sc., Ph.D., and D.Sc. degrees in radio communication from the Gdańsk University of Technology (Gdańsk Tech), Poland, in 2008, 2013, and 2020, respectively. Since 2008, he has been with the Department of Radiocommunication Systems and Networks, Gdańsk Tech, as a Research Assistant, during 2008–2013, as an Assistant Professor, during 2013–2020, and as an Associate Professor, since 2020. He participated and still participates in several projects related to special application of wireless techniques as well as three COST Actions (IC1004, CA15104, and CA20120). He is the author or coauthor of many publications, including book, book chapters, articles, reports, and papers presented during international and domestic conferences. His main scope of research is radio channel modeling in body area networks. His research interests include wireless communications and radio wave propagation. He is a Senior Member of URSI and a member of the Gdańsk Scientific Society. He is also a member of the European Association on Antennas and Propagation (EurAAP) Delegate Assembly, a Management Committee Member of the COST CA20120 Action, and a Vice-Chair of Commission-F of the Polish National Committee of URSI. In previous years, he was a member of the Board of the Working Group on Propagation of EurAAP, a Management Committee Substitute Member of the COST CA15104 Action, and the Chair of the Sub Working Group Internet-of-Things for Health within this action. He was a recipient of the Young Scientists Awards of URSI in 2016 and 2011, the Eighth International Conference on Wireless and Mobile Communications Best Paper Award in 2012, and many domestic awards.

KRZYSZTOF K. CWALINA (Member, IEEE) received the M.Sc.Eng. and Ph.D. degrees in telecommunication engineering from the Gdansk University of Technology, in 2014 and 2017, respectively. He is currently an Assistant Professor with the Department of Radiocommunication Systems and Networks. He has been a Contractor in six research and development projects mainly used in the field of national defense. He is the Head of the Project, realized in 2020–2023, co-financed under the European Regional Development Fund within the Smart Growth Operational. So far, he has conducted research mainly in the field of radio channel modeling, channel impulse response analysis, resource allocation in heterogeneous WBANs, and the use of UWB radio interface in indoor systems. His research interests include the issues of the artificial intelligence applications, in particular deep learning methods, in radiocommunication systems and networks. From 2016 to 2020, he was a member of the International IRACON project carried out as part of the COST CA15104 Action. In 2019, he was elected as an ERD of the European Association EURACON for a three-year term, in 2020–2022. He is a Senior Member of URSI. He was elected as the Junior Deputy Chairman of the Commission F in URSI Polish National Committee, in 2019. In 2021, he was elected as an URSI Early Career Representative of URSI Commission C for the period 2021–2026 and a member of the Board of the Working Group on Propagation of EurAAP.

PIOTR RAJCHOWSKI (Member, IEEE) was born in Poland, in 1989. He received the E.Eng., M.Sc., and Ph.D. degrees in radio communication from the Gdańsk University of Technology (Gdańsk Tech), Poland, in 2012, 2013, and 2017, respectively. Since 2013, he has been working at the Department of Radiocommunication Systems and Networks, Faculty of Electronics, Telecommunications and Informatics, Gdańsk University of Technology, as a IT Specialist, during 2013–2017, a Research Assistant, during 2017–2019, and as an Assistant Professor, since 2019. Since 2020, he has been the Deputy Head of the Department. His research and science activity include being the Contractor of six research and development projects related to homeland security, radiolocalization, and modern wireless networks. From 2019 to 2020, he was the Early Career Investigator Representative of the COST-IRACON CA-15104 Action, now he participates the CA20120 Action. His main research interests include radiolocalization in modern sensor and cellular networks. Moreover, he is interested in the aspects of the synchronization in the NB-IoT and 5G networks, especially in the harsh propagation conditions. He received the Young Scientists Award of URSI in 2020 and some domestic awards like the Annual Award of the President of the City of Gdańsk and the Gdańsk Scientific Society for Young Scientists.

FILIPE D. CARDOSO (Member, IEEE) received the Licenciado, M.Sc., and Ph.D. degrees in electrical and computer engineering from the IST/Technical University of Lisbon. Since 1994, he has been with the Department of Electrical Engineering, ESTSetúbal/Polytechnic Institute of Setúbal, Portugal, where he is currently a Tenured Professor of telecommunications and the Head of the Electronics and Telecommunications Area. He is also a Researcher at the INESC-ID, Lisbon. He was or is involved in European projects and networks of excellence COST 273, COST IC1004, COST CA15104, COST CA20120, IST/FLOWS, ICT/4WARD, ICT/EARTH, ICT/LEXNET, NEWCOM, and NEWCOM++. He was a Task Leader of Energy Efficiency in Transmission Techniques (EARTH) and Dissemination and Standardization (LEXNET) workgroups. He has authored papers in national and international conferences and journals, for which he has also served as a reviewer and a board member. His research interests include wireless/mobile channel characterization and modeling, body area networks, and mobile broadband systems. He was the Secretary of the IEEE ComSoc Portuguese Chapter.

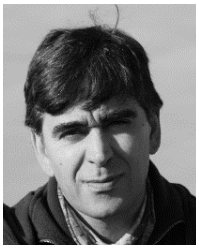

MANUEL M. FERREIRA (Member, IEEE) received the Licenciado degree in electronics and telecommunications from the University of Aveiro, and the M.Sc. degree in electrical and computer engineering from the IST/Technical University of Lisbon. Since 1995, he has been with the Department of Electrical Engineering, ESTSetúbal/Polytechnic Institute of Setúbal, Portugal, where he is currently a Professor of telecommunications and electronics. He was involved in European projects and networks of excellence COST CA20120, COST CA15104, NEWCOM, and ICT/LEXNET. His research interests include wireless/mobile channel characterization and wireless sensor and body area networks.

LUIS M. CORREIA (Senior Member, IEEE) was born in Portugal, in 1958. He received the Ph.D. degree in electrical and computer engineering from the IST, University of Lisbon, in 1991. He is currently a Professor of telecommunications with the IST, University of Lisbon, with his work focused on wireless and mobile communications, with the research activities developed in the INESC-ID Institute. He is an Honorary Professor of the Gdańsk University of Technology, Poland. He has acted as a Consultant for the Portuguese telecommunications operators and regulator, besides other public and private entities, and has been in the Board of Directors of a telecommunications company. He has participated in 32 projects within European frameworks, having coordinated six and taken leadership responsibilities at various levels in many others, besides national ones. He has supervised over 220 M.Sc./Ph.D. students, having edited six books, contribute to European strategic documents, and authored over 500 papers in international and national journals and conferences, for which served also as a reviewer, editor, and board member. Internationally, he was part of 37 Ph.D. juries, and 74 research projects and institutions evaluation committees for funding agencies in 12 countries, and the European Commission and COST. He was a recipient of the 2021 EurAAP Propagation Award for leadership in the field of propagation for wireless and mobile communications. He has been the Chairman of Conference, of the Technical Program Committee, and of the Steering Committee of 25 major conferences, besides other several duties. He was a National Delegate to the COST Domain Committee on ICT. He has launched and served as the Chairman for the IEEE Communications Society Portugal Chapter, besides being involved in several other duties in this society at the global level.